JACS
JOURNAL OF THE AMERICAN CHEMICAL SOCIETY
pubs.acs.org/JACS

Communication

Molecular Design for Optically Induced Magnetization: Targeting Excited State Orbital Degeneracy in Tungsten(V) Complexes

Ian E. Ramsier, Alysia Mandato, Sunil Saxena, and Wesley J. Transue*

Cite This: J. Am. Chem. Soc. 2025, 147, 18424−18430

ABSTRACT: The rise of quantum information science has spurred chemists to prepare new molecules that serve as useful building blocks in quantum technologies of the future. Implementation of molecular spin-based qubits requires new methods to induce high spin polarization of samples. Herein, we report design criteria to develop axially symmetric spin-1/2 molecules amenable to optically induced magnetization (OIM), a technique using circularly polarized (CP) excitation to deliver spin polarization. We apply these criteria to develop a series of tungsten(V) chalcogenide complexes that are demonstrated to have large spin-sensitive responses to CP light using magnetic circular dichroism (MCD) that could allow up to ∼20% spin polarization through OIM. Pulsed electron paramagnetic resonance (EPR) spectra reveal these systems have improved relaxation times over molecules like K_2IrCl_6, a species recently investigated by OIM, and field-swept electron spin−echo (FS-ESE) experiments show they have a remarkable lack of anisotropy in their phase-memory T_m times. The design criteria are general and point toward future ways to improve OIM-initializable qubits.

The development of molecular spin-based qubits[1] requires that spins fulfill several criteria outlined by DiVincenzo for quantum computing[2] or Degen for quantum sensing.[3] Of these criteria, use of molecular spin most prominently demands advancement in methods of "initialization," the process of selective spin polarization into a pure $|0\rangle$ or $|1\rangle$ state. Spin polarization is usually done thermally: application of an external magnetic field splits the M_S levels, and a Boltzmann population of these levels is then achieved on the timescale of the spin−lattice (T_1) relaxation time.[4] Conceptually, greater spin polarization can be easily reached by applying a larger magnetic field or cooling a sample further.[5] Practically, this is difficult. The combination of low temperatures and high fields does provide high polarization, but such instrumentation[6] can be prohibitively costly, and cooling below helium temperatures can cause increasingly slow T_1 relaxation.[7,8]

Nonthermal ways to polarize spin sidestep these issues, and optical methods have proven especially promising.[9−11] These techniques leverage electronic excitation and molecular design to influence spin, allowing chemists to untether spin polarization from Boltzmann population and spin T_1 relaxation. We are interested in a spin-sensitive optical phenomenon known as "optically induced magnetization" (OIM). OIM is deeply intertwined with a technique more familiar to chemists, magnetic circular dichroism (MCD): MCD measures the differential response of M_S levels to circularly polarized (CP) light ($\Delta\epsilon = \epsilon_{LCP} - \epsilon_{RCP}$),[12,13] whereas OIM exploits this differential response to preferentially bleach one M_S level. Despite demonstration of OIM in a wide variety of systems,[14−18] the method has not been well-explored to manipulate molecular spin. This will surely change after a recent report demonstrating the usefulness of OIM to explore ultrafast spin dynamics of K_2IrCl_6.[19]

Selection of K_2IrCl_6 relied on its octahedral geometry and its $^2T_{2g}$ ground state (GS) orbital angular momentum (OAM), promoting a large MCD/OIM response but also causing exceedingly short coherence (phase-memory) T_m times, even at 20 K.[19] Such rapid decoherence impairs many applications in quantum technologies by limiting the computations that can be performed or the information that may be sensed by a qubit.[2,3] Herein, we report a more flexible molecular design strategy to optimize OIM responses that allows us to explore the preparation of $S = 1/2$ molecules of axial symmetry that lack any GS OAM. Our design strategy led us to a series of tungsten(V) chalcogenide complexes $[\mathbf{1}\cdot E]^-$ (Figure 1a) that could give up to ∼20% spin polarization by OIM. Pulsed electron paramagnetic resonance (EPR) experiments reveal improved spin relaxation characteristics for these complexes due to their lack of GS OAM or a low-lying excited state (ES), and field-swept electron spin−echo (FS-ESE)[21] EPR measurements reveal a remarkable insensitivity of phase-memory (T_m) times to magnetic field.

Using the language of MCD theory, maximization of OIM is equivalent to maximization of the "C term" MCD response, something driven by spin−orbit coupling (SOC) in transition-metal systems.[22] The K_2IrCl_6 system experienced strong SOC due to the residual ("fictitious")[4] OAM in its GS, but there is no reason SOC splitting must come from the GS. Instead, we were inspired by ruby, where OIM can be performed from its

Received: March 3, 2025
Revised: April 17, 2025
Accepted: May 12, 2025
Published: May 20, 2025

https://doi.org/10.1021/jacs.5c03783
J. Am. Chem. Soc. 2025, 147, 18424−18430

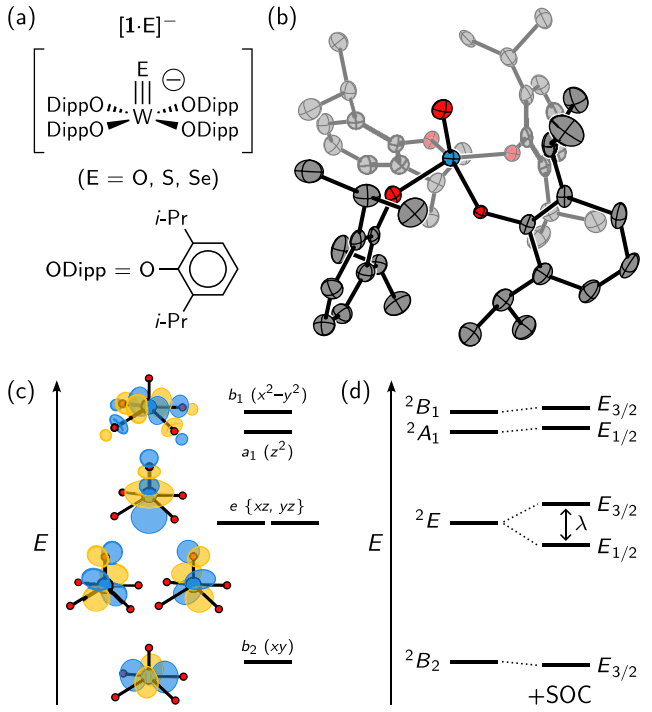

Figure 1. (a) The $[\mathbf{1}\cdot\mathrm{E}]^-$ compounds have bulky aryloxide ligands that enforce pseudo-C_{4v} geometry, confirmed by (b) the crystal structure of $[\mathrm{Na(THF)_6}][\mathbf{1}\cdot\mathrm{O}]$. (c) The *d* orbital splittings for $[\mathbf{1}\cdot\mathrm{O}]^-$ are shown with C_{4v} irrep labels. (d) SOC splits the ^2E state into two components labeled by C_{4v}^* double group irreps.[20]

orbitally nondegenerate $^4A_2$ GS to a degenerate ^2E ES.[14] This ^2E ES of ruby lacks residual OAM; yet, SOC still causes splitting into two Kramers doublets. Because SOC is the dominant driver of this splitting, spin and orbital angular momenta strongly mix to deliver a highly M_S-selective MCD/OIM response.[23] Clearly, threefold orbital degeneracy is not required for OIM.

Simply put, any point group possessing degenerate irreducible representations (irreps) may allow for orbital-based optimization of OIM. This certainly includes cubic point groups (O_h, T_d, etc.), but also all axial point groups of threefold-or-higher symmetry. At its simplest, OIM maximization should therefore incorporate

- axial ($C_{(n\geq 3)(v/h)}$, $D_{(n\geq 3)(h)}$, $D_{(n\geq 2)d}$, $S_{2n\geq 4}$) or isometric ($T_{(d/h)}$, $O_{(h)}$, $I_{(h)}$) point groups
- an optical transition involving an orbitally degenerate state
- SOC splitting of similar or greater magnitude to the line width of the electronic transition

.[18] An OIM-initializable qubit should additionally target increased spin coherence through

- avoidance of GS OAM and low-lying ESs
- a large absorptivity (ϵ) to allow more dilute samples

Of the few examples of molecular OIM we are aware of,[18,19] every system fails to satisfy at least one of these five criteria.

We selected tungsten(V)−oxo complex $[\mathbf{1}\cdot\mathrm{O}]^-$ as a promising system: tetragonal d^1 oxos generally have a low-lying ^2E ES (Figure 1c),[24] and 5*d* metals have strong SOC ($\zeta_{W(V)}$ = 3483 cm^{-1}).[25] Heating a THF solution of $WOCl_3(THF)_2$[26] and sodium 2,6-diisopropylphenoxide (NaODipp, 4 equiv) overnight (69 °C, 18 h) provided deep blue $[\mathrm{Na(THF)_6}][\mathbf{1}\cdot\mathrm{O}]$ in 50% recrystallized yield. A preliminary X-ray diffraction study (Figure 1b) revealed a nearly C_4-symmetric anion with a geometry close to an ideal square pyramid (τ_5 = 0.052(6)).[27] An optical $^2B_2 \rightarrow {}^2E$ transition was observed in the UV−vis−NIR absorption spectrum (16 100 cm^{-1}, Figure 2a) with a prominent shoulder due to tungsten(V) SOC, and a relatively large absorptivity for a *d*−*d* transition (270 M^{-1} cm^{-1}). Thus, $[\mathbf{1}\cdot\mathrm{O}]^-$ satisfied all our design requirements.

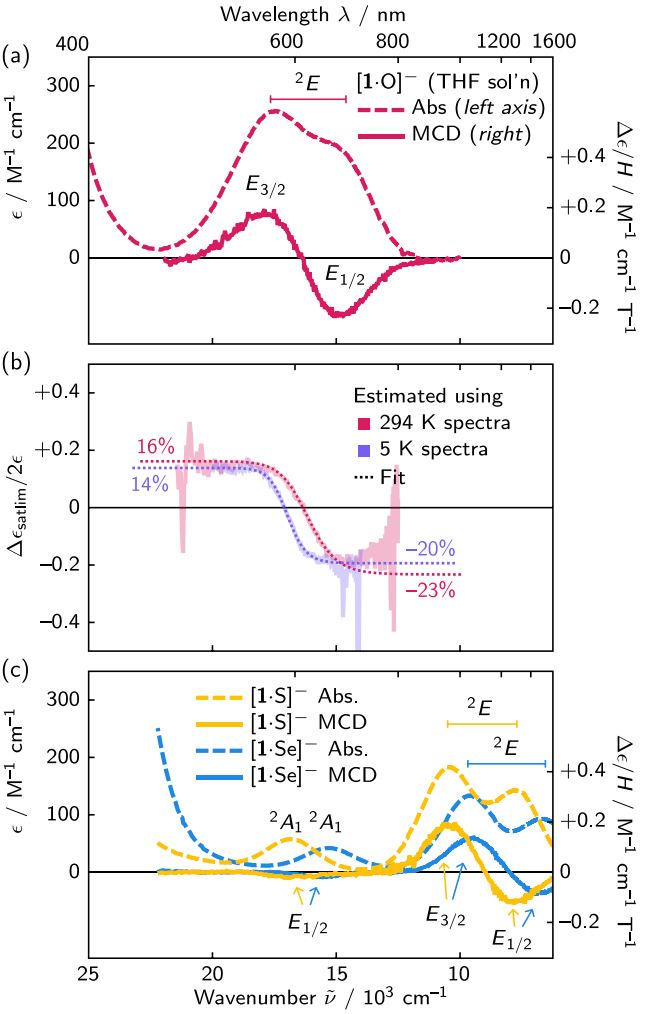

Figure 2. (a) Room-temperature UV−vis−NIR absorption and MCD spectra of $[\mathrm{Na(THF)_6}][\mathbf{1}\cdot\mathrm{O}]$ (THF solution). (b) The maximum spin polarization through OIM is $|\Delta\epsilon_{satlim}/2\epsilon|$, estimated here for $[\mathbf{1}\cdot\mathrm{O}]^-$ in two ways (see text and the SI). (c) The absorption and MCD spectra of the heavier chalcogenide complexes reveal a $^2A_1$ transition.

We were pleased to find the MCD spectrum of $[\mathbf{1}\cdot\mathrm{O}]^-$ shows large intensities associated with its ^2E ES. The SOC splitting of this state was clearly indicated by the characteristic bisignate ("pseudo-*A*") line shape, the negative and positive features corresponding to $E_{1/2}$ and $E_{3/2}$ levels, respectively (see the SI). The MCD intensities of these levels were quantified through their "C_0/D_0" ratios, a ratio of MCD *C* term intensity ("C_0") to absorption intensity ("D_0"). For a simple spin-1/2 GS lacking OAM and low-lying ESs, the maximum possible magnitude of $|C_0/D_0|$ is $g/2$, half the GS *g* value (see the derivation given in the SI); however, molecules typically feature ratios far smaller (Chart 1). The values for the $[\mathbf{1}\cdot\mathrm{O}]^-$

https://doi.org/10.1021/jacs.5c03783
J. Am. Chem. Soc. 2025, 147, 18424−18430

Chart 1. $^2B_2 \rightarrow {}^2E$ Transitions of $[\mathbf{1}\cdot\mathrm{E}]^-$ Species Have Far Stronger MCD Intensities than Other $S = 1/2$ Organic or Transition Metal Species with Smaller SOC; Their C_0/D_0 Ratios Approach Those of $[IrCl_6]^{2-}$, a System with GS OAM

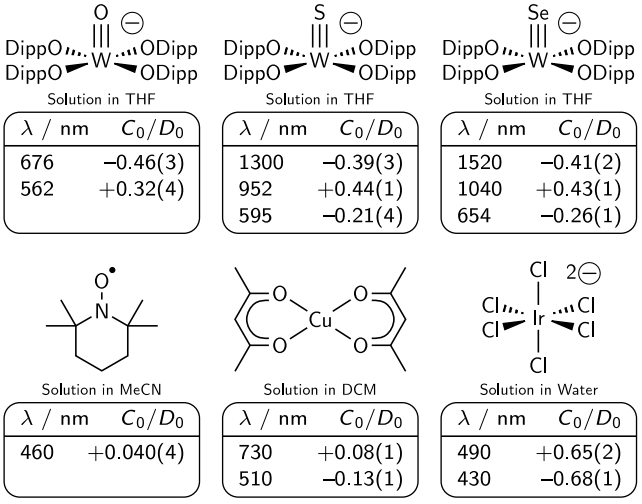

$^2B_2 \rightarrow {}^2E$ transitions (−0.46(3) and +0.32(4)) were quite large, multiple times larger than those of TEMPO$^\bullet$ and $Cu(acac)_2$ exemplars, and approach the values for $[IrCl_6]^{2-}$,[13,28] an ion specifically chosen for OIM studies due to its residual GS OAM.[19]

The MCD C_0/D_0 ratio is a useful heuristic, but more direct insight for OIM would come from measuring $\Delta\epsilon$ for each individual M_S level. This can be accomplished in the saturation limit. Magnetic saturation occurs under sufficiently low temperatures or high fields that most molecules populate a single M_S level. In the limit of complete saturation, the MCD spectrum reveals the intrinsic $\Delta\epsilon$ for the single lowest-energy M_S level. MCD intensity in the presence of saturation is nonlinear,[29]

$$\frac{\Delta\epsilon}{E} = \gamma\frac{2C_0}{g}\tanh\left(\frac{g\mu_B B}{2k_B T}\right)f(E) \qquad (1)$$

where E is the excitation energy, γ a proportionality constant, μ_B the Bohr magneton, B the magnetic field, k_B the Boltzmann constant, T the temperature, and $f(E)$ a line shape function (see the SI). We used eq 1 to estimate MCD in the saturation limit $\Delta\epsilon_{satlim}$ in two ways: from room-temperature data, and from cryogenic MCD data (5 K, 7 T). The maximum spin polarization that can be achieved by OIM is $|\Delta\epsilon_{satlim}/2\epsilon|$ (see the SI), and both methods of estimating $\Delta\epsilon_{satlim}/2\epsilon$ reveal that CP excitation of the $^2B_2 \rightarrow {}^2E$ transition can deliver up to 15% ($E_{3/2}$) or 20% ($E_{1/2}$) spin polarization, depending on wavelength of excitation (Figure 2b). For context, such a large polarization can only be achieved thermally at 1−1.5 K in X-band EPR experiments.

Analogous chalcogen congeners $[\mathbf{1}\cdot\mathrm{S}]^-$ and $[\mathbf{1}\cdot\mathrm{Se}]^-$ were also synthesized to explore their MCD intensities. The former was prepared by treating $W(ODipp)_4$[30] with $NaSCPh_3$ (1 equiv, THF), a convenient source of $S^{\bullet-}$ upon release of $CPh_3^\bullet$. Stirring overnight then washing with ether provided teal $[Na(THF)_6][\mathbf{1}\cdot\mathrm{S}]$ in 36% yield after recrystallization. The latter complex was prepared in a two-step one-pot procedure: $W(ODipp)_4$ was first treated with PPh_3Se to form the terminal selenide complex, and then reduction with $NaCPh_3$ formed the tungsten(V) anion. Recrystallization provided vibrant green $[Na(THF)_x(Et_2O)_y][\mathbf{1}\cdot\mathrm{Se}]$ in 26% isolated yield.

The MCD spectra of $[\mathbf{1}\cdot\mathrm{S/Se}]^-$ show the appearance of the $^2B_2 \rightarrow {}^2A_1$ ligand field transition, likely caused by weaker $\sigma_{W\equiv E}$ interactions in the heavier chalcogenides. This assignment follows from its negative MCD response, indicating $E_{1/2}$ symmetry, and is corroborated by model CASSCF/RI-NEVPT2 calculations (see the SI).[31] We ascribe the weaker $|C_0/D_0|$ ratios (Chart 1) of the $^2B_2 \rightarrow {}^2A_1$ transitions to a lack of ES orbital degeneracy. For such nondegenerate states, the sum-over-states perturbation theory formalism[22] says C term intensity is proportional to the reciprocal energy difference to other states coupling through SOC. This is an important distinction from ^2E states, underscoring that design of molecules with large MCD/OIM responses should target transitions involving orbital degeneracy.

All three chalcogenide complexes can be observed by continuous-wave (CW) EPR experiments at temperatures at least up to 80 K due to their lack of GS OAM and thus slower

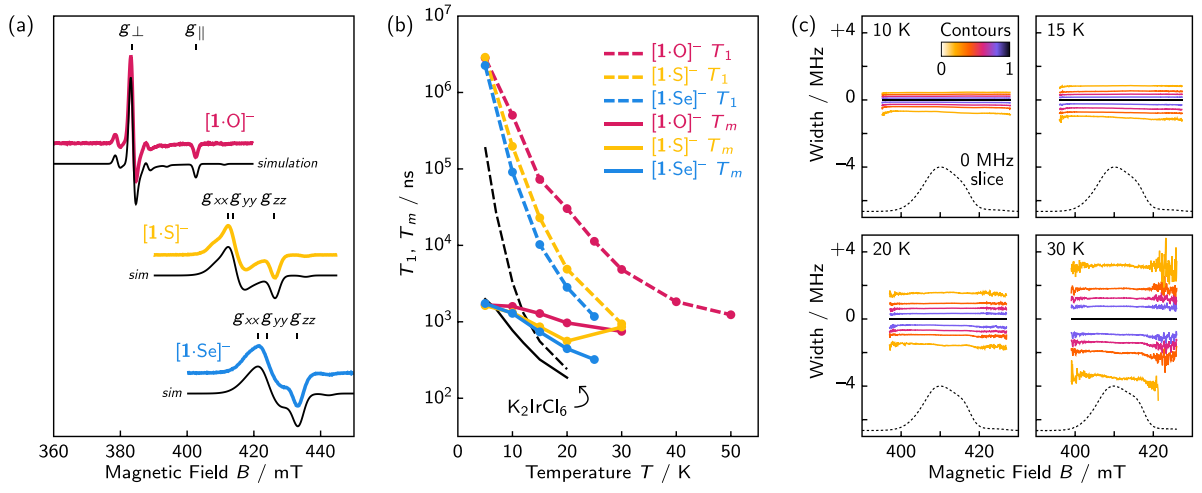

Figure 3. (a) The CW EPR spectra show approximate C_4 symmetry for all anions with slight rhombic distortions for $[\mathbf{1}\cdot\mathrm{S/Se}]^-$. (b) Spin T_1 and T_m measurements show slower relaxation for $[\mathbf{1}\cdot\mathrm{E}]^-$ anions than K_2IrCl_6 (values from ref 19) due to the latter's GS OAM. (c) Normalized contours in the FS-ESE spectrum of $[\mathbf{1}\cdot\mathrm{Se}]^-$ show nearly flat T_m times independent of field.

https://doi.org/10.1021/jacs.5c03783
J. Am. Chem. Soc. 2025, 147, 18424−18430

relaxation properties. Inversion recovery and Hahn-echo X-band EPR experiments were used to directly measure T_1 and T_m times (Figure 3), giving values higher than those of K_2IrCl_6 (10−100 times higher at 20 K);[19] in fact, even higher values may be attainable through techniques like deuteration,[32] picket-fence saturation recovery experiments,[33] and Carr−Purcell−Meiboom−Gill (CPMG) pulse sequences.[34] Despite this increase in coherence for $[\mathbf{1}\cdot E]^-$ complexes, these T_m relaxation times are still modest likely due to the strong SOC within the systems.[35] A balance clearly needs to be struck between maximizing MCD/OIM using heavy atom SOC while avoiding the collapse of spin coherence, and this will be a fascinating area for future exploration.

The T_1 and T_m measurements also showed unexpectedly consistent relaxation times when measured in the $g_\parallel$ and $g_\perp$ regions of the spectra. Such behavior differs from related species,[36] which often show large variations across the spectra.[37] This insensitivity to magnetic field was demonstrated using a 2D FS-ESE EPR experiment[21] conducted on $[\mathbf{1}\cdot Se]^-$, showing nearly constant T_m times across the entire spectrum. Studies are ongoing to uncover correlations between relaxation times, molecular symmetry, and MCD/OIM intensity.

With this work, we hope to highlight that a large synthetic space remains to be explored in the development of optimal molecules for OIM. Our results ease the restrictive O_h design strategy for OIM, showing that chemists can exploit axial symmetry to deliver large MCD responses. This increased flexibility should allow targeting of other properties important for qubits, especially spin relaxation times. Ligand design may be particularly useful, as the ODipp ligands here were selected for ease of use[30] rather than promotion of spin coherence.[38−40] We are conducting experiments toward these ends, and toward balancing spin and optical lifetimes for future implementation of OIM in molecular qubit systems on the nanosecond time scale.[41]

■ ASSOCIATED CONTENT

Supporting Information

The Supporting Information is available free of charge at https://pubs.acs.org/doi/10.1021/jacs.5c03783.

Experimental details, spectroscopic characterization, crystallographic information, computational details, and theoretical derivations (PDF)

Accession Codes

Deposition Numbers 2428564−2428566 and 2444691 contain the supplementary crystallographic data for this paper. These data can be obtained free of charge via the joint Cambridge Crystallographic Data Centre (CCDC) and Fachinformationszentrum Karlsruhe Access Structures service.

■ AUTHOR INFORMATION

Corresponding Author

Wesley J. Transue − *Department of Chemistry, University of Pittsburgh, Pittsburgh, Pennsylvania 15213, United States;* orcid.org/0000-0001-7445-5663; Email: wtransue@pitt.edu

Authors

Ian E. Ramsier − *Department of Chemistry, University of Pittsburgh, Pittsburgh, Pennsylvania 15213, United States*

Alysia Mandato − *Department of Chemistry, University of Pittsburgh, Pittsburgh, Pennsylvania 15213, United States*

Sunil Saxena − *Department of Chemistry, University of Pittsburgh, Pittsburgh, Pennsylvania 15213, United States;* orcid.org/0000-0001-9098-6114

Complete contact information is available at: https://pubs.acs.org/10.1021/jacs.5c03783

Notes

The authors declare no competing financial interest.

■ ACKNOWLEDGMENTS

Financial support from the University of Pittsburgh (to W.J.T.) and NSF BSF MCB 2407706 (to S.S.) is gratefully acknowledged. We also thank Sydney Giles for help acquiring cryogenic data.

■ REFERENCES

(1) Wasielewski, M. R.; et al. Exploiting Chemistry and Molecular Systems for Quantum Information Science. *Nat. Rev. Chem.* **2020**, *4*, 490−504.

(2) DiVincenzo, D. P. The Physical Implementation of Quantum Computation. *Fortschr. Phys.* **2000**, *48*, 771−783.

(3) Degen, C. L.; Reinhard, F.; Cappellaro, P. Quantum Sensing. *Rev. Mod. Phys.* **2017**, *89*, 035002.

(4) Abragam, A.; Bleaney, B. *Electron Paramagnetic Resonance of Transition Ions*; Marshall, W., Wilkinson, D. H., Eds.; The International Series of Monographs on Physics; Oxford University Press: Oxford, U.K., 1970.

(5) Eaton, G. R.; Eaton, S. S.; Barr, D. P.; Weber, R. T. *Quantitative EPR*; Springer-Verlag: Wien, Austria and New York, 2010.

(6) (a) Rohrer, M.; Brügmann, O.; Kinzer, B.; Prisner, T. F. High-Field/High-Frequency EPR Spectrometer Operating in Pulsed and Continuous-Wave Mode at 180 GHz. *Appl. Magn. Reson.* **2001**, *21*, 257−274. (b) Hertel, M. M.; Denysenkov, V. P.; Bennati, M.; Prisner, T. F. Pulsed 180-GHz EPR/ENDOR/PELDOR Spectroscopy. *Magn. Reson. Chem.* **2005**, *43*, S248−S255.

(7) Eaton, S. S.; Eaton, G. R. Distance Measurements in Biological Systems by EPR. In *Biological Magnetic Resonance*; Berliner, L. J., Eaton, G. R., Eaton, S. S., Eds.; Springer US: Boston, MA, 2000; pp 29−154.

(8) X-band EPR experiences ∼5% population difference between MS levels at 4.2 K.

(9) (a) Chernick, E. T.; Mi, Q.; Kelley, R. F.; Weiss, E. A.; Jones, B. A.; Marks, T. J.; Ratner, M. A.; Wasielewski, M. R. Electron Donor-Bridge-Acceptor Molecules with Bridging Nitronyl Nitroxide Radicals: Influence of a Third Spin on Charge- and Spin-Transfer Dynamics. *J. Am. Chem. Soc.* **2006**, *128*, 4356−4364. (b) Colvin, M. T.; Giacobbe, E. M.; Cohen, B.; Miura, T.; Scott, A. M.; Wasielewski, M. R. Competitive Electron Transfer and Enhanced Intersystem Crossing in Photoexcited Covalent TEMPO-Perylene-3,4:9,10-Bis-(Dicarboximide) Dyads: Unusual Spin Polarization Resulting from the Radical-Triplet Interaction. *J. Phys. Chem. A* **2010**, *114*, 1741−1748. (c) Colvin, M. T.; Carmieli, R.; Miura, T.; Richert, S.; Gardner, D. M.; Smeigh, A. L.; Dyar, S. M.; Conron, S. M.; Ratner, M. A.; Wasielewski, M. R. Electron Spin Polarization Transfer from Photogenerated Spin-Correlated Radical Pairs to a Stable Radical Observer Spin. *J. Phys. Chem. A* **2013**, *117*, 5314−5325. (d) Wasielewski, M. R. Light-Driven Spin Chemistry for Quantum Information Science. *Phys. Today* **2023**, *76*, 28−34.

(10) (a) Stein, B. W.; Tichnell, C. R.; Chen, J.; Shultz, D. A.; Kirk, M. L. Excited State Magnetic Exchange Interactions Enable Large Spin Polarization Effects. *J. Am. Chem. Soc.* **2018**, *140*, 2221−2228. (b) Kirk, M. L.; Shultz, D. A.; Chen, J.; Hewitt, P.; Daley, D.; Paudel, S.; van der Est, A. Metal Ion Control of Photoinduced Electron Spin Polarization in Electronic Ground States. *J. Am. Chem. Soc.* **2021**, *143*, 10519−10523. (c) Kirk, M. L.; Shultz, D. A.; Marri, A. R.; Hewitt, P.; van der Est, A. Single-Photon-Induced Electron Spin Polarization of Two Exchange-Coupled Stable Radicals. *J. Am. Chem. Soc.* **2022**, *144*,

21005−21009. (d) Kirk, M. L.; Shultz, D. A.; Marri, A. R.; van der Est, A. Photoinduced Magnetic Exchange-Jump Promotes Ground State Biradical Electron Spin Polarization. *J. Am. Chem. Soc.* **2024**, *146*, 9285−9292.
(11) (a) Bayliss, S. L.; Laorenza, D. W.; Mintun, P. J.; Kovos, B. D.; Freedman, D. E.; Awschalom, D. D. Optically Addressable Molecular Spins for Quantum Information Processing. *Science* **2020**, *370*, 1309−1312. (b) Laorenza, D. W.; Kairalapova, A.; Bayliss, S. L.; Goldzak, T.; Greene, S. M.; Weiss, L. R.; Deb, P.; Mintun, P. J.; Collins, K. A.; Awschalom, D. D.; Berkelbach, T. C.; Freedman, D. E. Tunable Cr^{4+} Molecular Color Centers. *J. Am. Chem. Soc.* **2021**, *143*, 21350. (c) Bayliss, S. L.; Deb, P.; Laorenza, D. W.; Onizhuk, M.; Galli, G.; Freedman, D. E.; Awschalom, D. D. Enhancing Spin Coherence in Optically Addressable Molecular Qubits through Host-Matrix Control. *Phys. Rev. X* **2022**, *12*, 031028.
(12) Mason, W. R. *A Practical Guide to Magnetic Circular Dichroism Spectroscopy*, 1st Edition; John Wiley & Sons: Hoboken, NJ, 2007.
(13) Piepho, S. B.; Schatz, P. N. *Group Theory in Spectroscopy with Applications to Magnetic Circular Dichroism*; John Wiley & Sons: New York, 1983.
(14) (a) Hull, G. F.; Smith, J. T.; Quesada, A. F. Alignment of Cr^{3+} in Ruby. *Appl. Opt.* **1965**, *4*, 1117−1120. (b) Van Der Ziel, J. P.; Bloembergen, N. Optically Induced Magnetization in Ruby. *Phys. Rev.* **1965**, *138*, A1287−A1292. (c) Takagi, Y.; Fukuda, Y.; Yamada, K.; Hashi, T. Optical Excitation of Zeeman Coherence in Ruby. *J. Phys. Soc. Jpn.* **1981**, *50*, 2672−2681. (d) Takagi, Y.; Fukuda, Y.; Hashi, T. Optical Spin Orientation in Ruby by Zeeman-selective U-band Absorption. *Opt. Commun.* **1985**, *55*, 115−119.
(15) (a) Kolesov, R. Dynamics of Laser-Induced Magnetization in Ce-doped Yttrium Aluminum Garnet. *Phys. Rev. A* **2007**, *76*, 043831. (b) Kolesov, R.; Xia, K.; Reuter, R.; Jamali, M.; Stöhr, R.; Inal, T.; Siyushev, P.; Wrachtrup, J. Mapping Spin Coherence of a Single Rare-Earth Ion in a Crystal onto a Single Photon Polarization State. *Phys. Rev. Lett.* **2013**, *111*, 120502. (c) Siyushev, P.; Xia, K.; Reuter, R.; Jamali, M.; Zhao, N.; Yang, N.; Duan, C.; Kukharchyk, N.; Wieck, A. D.; Kolesov, R.; Wrachtrup, J. Coherent Properties of Single Rare-Earth Spin Qubits. *Nat. Commun.* **2014**, *5*, 3895. (d) Azamat, D. V.; Belykh, V. V.; Yakovlev, D. R.; Fobbe, F.; Feng, D. H.; Evers, E.; Jastrabik, L.; Dejneka, A.; Bayer, M. Electron Spin Dynamics of Ce^{3+} Ions in YAG Crystals Studied by Pulse-EPR and Pump-Probe Faraday Rotation. *Phys. Rev. B* **2017**, *96*, 075160. (e) Liang, P.; Hu, R. R.; Chen, C.; Belykh, V. V.; Jia, T. Q.; Sun, Z. R.; Feng, D. H.; Yakovlev, D. R.; Bayer, M. Room-Temperature Electron Spin Dynamics of Ce^{3+} Ions in a YAG Crystal. *Appl. Phys. Lett.* **2017**, *110*, 222405. (f) Liang, P.; Zhao, H.; Hu, R. Electron Spin Dynamics in Multi-Energy Level Systems under the Excitation of Circular Polarization Modulated Continuous-Wave Laser. *J. Lumin.* **2023**, *263*, 120082.
(16) Yakovlev, D. R.; Bayer, M. In *Spin Physics in Semiconductors*; Dyakonov, M. I., Ed.; Springer: Berlin, Heidelberg, 2008; pp 135−177.
(17) (a) Walker, T. G.; Happer, W. Spin-Exchange Optical Pumping of Noble-Gas Nuclei. *Rev. Mod. Phys.* **1997**, *69*, 629−642. (b) Saxena, S.; Wong-Foy, A.; Moule, A. J.; Seeley, J. A.; McDermott, R.; Clarke, J.; Pines, A. Resolution of ^{129}Xe Chemical Shifts at Ultralow Magnetic Field. *J. Am. Chem. Soc.* **2001**, *123*, 8133−8134. (c) Wong-Foy, A.; Saxena, S.; Moulé, A. J.; Bitter, H.-M. L.; Seeley, J. A.; McDermott, R.; Clarke, J.; Pines, A. Laser-Polarized ^{129}Xe NMR and MRI at Ultralow Magnetic Fields. *J. Magn. Reson.* **2002**, *157*, 235−241.
(18) (a) Takagi, Y. Optical Spin Orientation in Aqueous Solution of Manganese(II) Sulfate. *Optics Commun.* **1986**, *59*, 122−126. (b) Takagi, Y.; Miyazaki, S.; Ishikawa, K. Different Mechanisms of Impulsive Optical Spin Orientation in Paramagnetic and Diamagnetic Copper(II) Complexes. *Chem. Phys. Lett.* **2004**, *393*, 314−318. (c) Takagi, Y.; Miyazaki, S.; Minamihara, R.; Makino, T.; Fujimoto, K.; Yamada, J.-I.; Nakatsuji, S. Direct Detection of Optically-Induced Microwave Spin Precession in Fe(III) Halogenates. *J. Magn. Magn. Mater.* **2007**, *317*, 8−14. (d) Furue, S.; Nakayama, K.; Kohmoto, T.; Kunitomo, M.; Fukuda, Y. Quantum-Beat Free-Induction Decay of Copper Ions in an Aqueous Solution: Fourier-Transform ESR Spectroscopy by Optical Means. *Jpn. J. Appl. Phys.* **2004**, *43*, 2489. (e) Furue, S.; Kohmoto, T.; Kunitomo, M.; Fukuda, Y. Optical Induction of Magnetization and Observation of Fast Spin Dynamics in Aqueous Solutions of Copper Ions. *Phys. Lett. A* **2005**, *345*, 415−422.
(19) Sutcliffe, E.; Kazmierczak, N. P.; Hadt, R. G. Ultrafast All-Optical Coherence of Molecular Electron Spins in Room-Temperature Water Solution. *Science* **2024**, *386*, 888−892.
(20) Altmann, S. L.; Herzig, P. *Point-Group Theory Tables*, 2nd Edition; PHAIDRA−University of Vienna: Wien, Austria, 2011.
(21) (a) Millhauser, G. L.; Freed, J. H. Two-dimensional Electron Spin Echo Spectroscopy and Slow Motions. *J. Chem. Phys.* **1984**, *81*, 37−48. (b) Millhauser, G. L.; Freed, J. H. Linear Prediction and Resolution Enhancement of Complex Line Shapes in Two-dimensional Electron-spin-echo Spectroscopy. *J. Chem. Phys.* **1986**, *85*, 63−67.
(22) Neese, F.; Solomon, E. I. MCD *C*-Term Signs, Saturation Behavior, and Determination of Band Polarizations in Randomly Oriented Systems with Spin $S \geq 1/2$. Applications to $S = 1/2$ and $S = 5/2$. *Inorg. Chem.* **1999**, *38*, 1847−1865.
(23) (a) Trabjerg, I.; Güdel, H. U.; Svendsen, E. N.; Østvold, T.; Bjørseth, A.; Powell, D. L. Absorption of Circularly Polarized Light by the $^4A_2 \rightarrow {}^2E$ and $^4A_2 \rightarrow {}^2T_2$ Transitions of Ruby in Strong Magnetic Fields, I. *Acta Chem. Scand.* **1974**, *28a*, 8−12. (b) Trabjerg, I.; Larsen, E.; Moreira, J. E.; Nielsen, O. F.; Skoglund, U. Absorption of Circularly Polarized Light by the $^2E \leftarrow {}^4A_2$ and $^2T_2 \leftarrow {}^4A_2$ Transitions in Ruby in Strong Magnetic Fields, II. *Acta Chem. Scand. A* **1975**, *29*, 817−823.
(24) (a) Ballhausen, C. J.; Gray, H. B. The Electronic Structure of the Vanadyl Ion. *Inorg. Chem.* **1962**, *1*, 111−122. (b) Robbins, D. J.; Stillman, M. J.; Thomson, A. J. Magnetic Circular Dichroism Spectroscopy of the Vanadyl Ion. *J. Chem. Soc., Dalton Trans.* **1974**, 813−820. (c) Sabel, D. M.; Gewirth, A. A. Magnetic Circular Dichroism Studies of Metal Oxytetrachloride (Metal = Chromium, Molybdenum, Tungsten) Chromophores: Assignment of Ligand Field and Charge Transfer States. *Inorg. Chem.* **1994**, *33*, 148−156. (d) Van Stappen, C.; Maganas, D.; DeBeer, S.; Bill, E.; Neese, F. Investigations of the Magnetic and Spectroscopic Properties of V(III) and V(IV) Complexes. *Inorg. Chem.* **2018**, *57*, 6421−6438.
(25) Bendix, J.; Brorson, M.; Schaffer, C. E. Accurate Empirical Spin−Orbit Coupling Parameters Z_{nd} for Gaseous Nd^q Transition Metal Ions. The Parametrical Multiplet Term Model. *Inorg. Chem.* **1993**, *32*, 2838−2849.
(26) Persson, C.; Andersson, C. Reduction of Tungsten(VI) and Molybdenum(V) by Allyltrimethylsilane and Cyclopentene. Simple High Yield Syntheses of $MoCl_4(OEt_2)_2$, $MoCl_4(DME)$, $WCl_4(THF)_2$, $WCl_4(DME)$ and $WOCl_3(THF)_2$. *Inorg. Chim. Acta* **1993**, *203*, 235−238.
(27) Addison, A. W.; Rao, T. N.; Reedijk, J.; van Rijn, J.; Verschoor, G. C. Synthesis, Structure, and Spectroscopic Properties of Copper(II) Compounds Containing Nitrogen−Sulphur Donor Ligands; the Crystal and Molecular Structure of Aqua[1,7-Bis(*N*-Methylbenzimidazol-2′-yl)-2,6-Dithiaheptane]Copper(II) Perchlorate. *J. Chem. Soc., Dalton Trans.* **1984**, *0*, 1349−1356.
(28) Henning, G. N.; McCaffery, A. J.; Schatz, P. N.; Stephens, P. J. Magnetic Circular Dichroism of Charge-Transfer Transitions: Low-Spin d^5 Hexahalide Complexes. *J. Chem. Phys.* **1968**, *48*, 5656−5661.
(29) Stephens, P. J. Magnetic Circular Dichroism. *Adv. Chem. Phys.* **1976**, *35*, 197−264.
(30) (a) Listemann, M. L.; Dewan, J. C.; Schrock, R. R. Monomeric Tungsten(IV) Phenoxide and Thiolate Complexes. *J. Am. Chem. Soc.* **1985**, *107*, 7207−7208. (b) Listemann, M. L.; Schrock, R. R.; Dewan, J. C.; Kolodziej, R. M. Synthesis and Reactivity of Two Monomeric Tungsten(IV) Phenoxide Complexes. *Inorg. Chem.* **1988**, *27*, 264−271. (c) Joost, M.; Transue, W. J.; Cummins, C. C. Terminal Tungsten Pnictide Complex Formation through Pnictaethynolate Decarbonylation. *Chem. Commun.* **2017**, *53*, 10731−10733. (d) Joost, M.; Transue, W. J.; Cummins, C. Diazomethane Umpolung atop

https://doi.org/10.1021/jacs.5c03783
J. Am. Chem. Soc. 2025, 147, 18424−18430

Anthracene: An Electrophilic Methylene Transfer Reagent. *Chem. Sci.* **2018**, *9*, 1540−1543.
(31) (a) Neese, F. Software Update: The ORCA Program System, Version 4.0. *WIREs Comput. Mol. Sci.* **2018**, *8*, No. e1327. (b) Ganyushin, D.; Neese, F. First-Principles Calculations of Zero-Field Splitting Parameters. *J. Chem. Phys.* **2006**, *125*, 024103. (c) Stoychev, G. L.; Auer, A. A.; Neese, F. Automatic Generation of Auxiliary Basis Sets. *J. Chem. Theory Comput.* **2017**, *13*, 554−562. (d) Kollmar, C.; Sivalingam, K.; Helmich-Paris, B.; Angeli, C.; Neese, F. A Perturbation-Based Super-CI Approach for the Orbital Optimization of a CASSCF Wave Function. *J. Comput. Chem.* **2019**, *40*, 1463−1470. (e) Lang, L.; Neese, F. Spin-Dependent Properties in the Framework of the Dynamic Correlation Dressed Complete Active Space Method. *J. Chem. Phys.* **2019**, *150*, 104104. (f) Kollmar, C.; Sivalingam, K.; Guo, Y.; Neese, F. An Efficient Implementation of the NEVPT2 and CASPT2Methods Avoiding Higher-Order Density Matrices. *J. Chem. Phys.* **2021**, *155*, 234104. (g) Guo, Y.; Sivalingam, K.; Neese, F. Approximations of Density Matrices in N-electron Valence State Second-Order Perturbation Theory (NEVPT2). I. Revisiting the NEVPT2 Construction. *J. Chem. Phys.* **2021**, *154*, 214111.
(32) (a) Eaton, G. R.; Eaton, S. S. Solvent and Temperature Dependence of Spin Echo Dephasing for Chromium(V) and Vanadyl Complexes in Glassy Solution. *J. Magn. Reson.* **1999**, *136*, 63−68. (b) Ward, R.; Bowman, A.; Sozudogru, E.; El-Mkami, H.; Owen-Hughes, T.; Norman, D. G. EPR Distance Measurements in Deuterated Proteins. *J. Magn. Reson.* **2010**, *207*, 164−167. (c) El Mkami, H.; Ward, R.; Bowman, A.; Owen-Hughes, T.; Norman, D. G. The Spatial Effect of Protein Deuteration on Nitroxide Spin-Label Relaxation: Implications for EPR Distance Measurement. *J. Magn. Reson.* **2014**, *248*, 36−41. (d) El Mkami, H.; Norman, D. G. Spin Probes, and Intrinsic Metal Ions. In *Electron Paramagnetic Resonance Investigations of Biological Systems by Using Spin Labels, Part B*; Qin, P. Z., Warncke, K., Eds.; Methods in Enzymology, Vol. *564*; Academic Press, 2015; pp 125−152. (e) Schmidt, T.; Wälti, M. A.; Baber, J. L.; Hustedt, E. J.; Clore, G. M. Long Distance Measurements up to 160 Å in the GroEL Tetradecamer Using Q-Band DEER EPR Spectroscopy. *Angew. Chem., Int. Ed.* **2016**, *55*, 15905−15909. (f) Casto, J.; Mandato, A.; Saxena, S. dHis-troying Barriers: Deuteration Provides a Pathway to Increase Sensitivity and Accessible Distances for Cu^{2+} Labels. *J. Phys. Chem. Lett.* **2021**, *12*, 4681−4685.
(33) (a) Cernescu, A.; Maly, T.; Prisner, T. F. 2D-REFINE Spectroscopy: Separation of Overlapping Hyperfine Spectra. *J. Magn. Reson.* **2008**, *192*, 78−84. (b) McPeak, J.; Alexander, D.; Joseph, C.; Eaton, S. S.; Eaton, G. R. Electron Spin Relaxation of Tb^{3+} and Tm^{3+} Ions. *Appl. Magn. Reson.* **2020**, *51*, 961−976. (c) Kazmierczak, N. P.; Oyala, P. H.; Hadt, R. G. Spectroscopic Signatures of Phonon Character in Molecular Electron Spin Relaxation. *ACS Cent. Sci.* **2024**, *10*, 2353−2362.
(34) (a) Eliav, U.; Freed, J. H. Multipulse Sequences in Electron-spin Echoes. *Rev. Sci. Instrum.* **1983**, *54*, 1416−1417. (b) Harbridge, J. R.; Eaton, S. S.; Eaton, G. R. Comparison of Electron Spin Relaxation Times Measured by Carr−Purcell−Meiboom−Gill and Two-Pulse Spin-Echo Sequences. *J. Magn. Reson.* **2003**, *164*, 44−53. (c) Mentink-Vigier, F.; Collauto, A.; Feintuch, A.; Kaminker, I.; Tarle, V.; Goldfarb, D. Increasing Sensitivity of Pulse EPR Experiments Using Echo Train Detection Schemes. *J. Magn. Reson.* **2013**, *236*, 117−125. (d) Zaripov, R.; Vavilova, E.; Miluykov, V.; Bezkishko, I.; Sinyashin, O.; Salikhov, K.; Kataev, V.; Büchner, B. Boosting the Electron Spin Coherence in Binuclear Mn Complexes by Multiple Microwave Pulses. *Phys. Rev. B* **2013**, *88*, 094418.
(35) (a) Graham, M. J.; Zadrozny, J. M.; Shiddiq, M.; Anderson, J. S.; Fataftah, M. S.; Hill, S.; Freedman, D. E. Influence of Electronic Spin and Spin−Orbit Coupling on Decoherence in Mononuclear Transition Metal Complexes. *J. Am. Chem. Soc.* **2014**, *136*, 7623−7626. (b) Pearson, T. J.; Laorenza, D. W.; Krzyaniak, M. D.; Wasielewski, M. R.; Freedman, D. E. Octacyanometallate Qubit Candidates. *Dalton Trans.* **2018**, *47*, 11744−11748.
(36) Husted, R.; Du, J.-L.; Eaton, G. R.; Eaton, S. S. Temperature and Orientation Dependence of Electron Spin Relaxation in Molybdenum(V) Porphyrins. *Magn. Reson. Chem.* **1995**, *33*, S66−S69.
(37) (a) Kazmierczak, N. P.; Hadt, R. G. Illuminating Ligand Field Contributions to Molecular Qubit Spin Relaxation via T_1 Anisotropy. *J. Am. Chem. Soc.* **2022**, *144*, 20804−20814. (b) Kazmierczak, N. P.; Luedecke, K. M.; Gallmeier, E. T.; Hadt, R. G. T_1 Anisotropy Elucidates Spin Relaxation Mechanisms in an $S = 1$ Cr(IV) Optically Addressable Molecular Qubit. *J. Phys. Chem. Lett.* **2023**, *14*, 7658−7664.
(38) (a) Fataftah, M. S.; Zadrozny, J. M.; Rogers, D. M.; Freedman, D. E. A Mononuclear Transition Metal Single-Molecule Magnet in a Nuclear Spin-Free Ligand Environment. *Inorg. Chem.* **2014**, *53*, 10716−10721. (b) Zadrozny, J. M.; Niklas, J.; Poluektov, O. G.; Freedman, D. E. Millisecond Coherence Time in a Tunable Molecular Electronic Spin Qubit. *ACS Cent. Sci.* **2015**, *1*, 488−492. (c) Zadrozny, J. M.; Freedman, D. E. Qubit Control Limited by Spin−Lattice Relaxation in a Nuclear Spin-Free Iron(III) Complex. *Inorg. Chem.* **2015**, *54*, 12027−12031. (d) Yu, C.-J.; Graham, M. J.; Zadrozny, J. M.; Niklas, J.; Krzyaniak, M. D.; Wasielewski, M. R.; Poluektov, O. G.; Freedman, D. E. Long Coherence Times in Nuclear Spin-Free Vanadyl Qubits. *J. Am. Chem. Soc.* **2016**, *138*, 14678−14685. (e) Graham, M. J.; Yu, C.-J.; Krzyaniak, M. D.; Wasielewski, M. R.; Freedman, D. E. Synthetic Approach To Determine the Effect of Nuclear Spin Distance on Electronic Spin Decoherence. *J. Am. Chem. Soc.* **2017**, *139*, 3196−3201. (f) Amdur, M. J.; Mullin, K. R.; Waters, M. J.; Puggioni, D.; Wojnar, M. K.; Gu, M.; Sun, L.; Oyala, P. H.; Rondinelli, J. M.; Freedman, D. E. Chemical Control of Spin−Lattice Relaxation to Discover a Room Temperature Molecular Qubit. *Chem. Sci.* **2022**, *13*, 7034−7045.
(39) (a) Lin, C.-Y.; Ngendahimana, T.; Eaton, G. R.; Eaton, S. S.; Zadrozny, J. M. Counterion Influence on Dynamic Spin Properties in a V(IV) Complex. *Chem. Sci.* **2019**, *10*, 548−555. (b) Jackson, C. E.; Lin, C.-Y.; Johnson, S. H.; van Tol, J.; Zadrozny, J. M. Nuclear-Spin-Pattern Control of Electron-Spin Dynamics in a Series of V(IV) Complexes. *Chem. Sci.* **2019**, *10*, 8447−8454. (c) Campanella, A. J.; Nguyen, M.-T.; Zhang, J.; Ngendahimana, T.; Antholine, W. E.; Eaton, G. R.; Eaton, S. S.; Glezakou, V.-A.; Zadrozny, J. M. Ligand Control of Low-Frequency Electron Paramagnetic Resonance Linewidth in Cr(III) Complexes. *Dalton Trans.* **2021**, *50*, 5342−5350. (d) Jackson, C. E.; Ngendahimana, T.; Lin, C.-Y.; Eaton, G. R.; Eaton, S. S.; Zadrozny, J. M. Impact of Counter Ion Methyl Groups on Spin Relaxation in $[V(C_6H_4O_2)_3]^{2-}$. *J. Phys. Chem. C* **2022**, *126*, 7169−7176. (e) Martinez, R.; Jackson, C. E.; Üngör, Ö.; van Tol, J.; Zadrozny, J. M. Impact of Ligand Chlorination and Counterion Tuning on High-Field Spin Relaxation in a Series of V(IV) Complexes. *Dalton Trans.* **2023**, *52*, 10805−10816.
(40) (a) Mirzoyan, R.; Hadt, R. G. The Dynamic Ligand Field of a Molecular Qubit: Decoherence through Spin−Phonon Coupling. *Phys. Chem. Chem. Phys.* **2020**, *22*, 11249−11265. (b) Mirzoyan, R.; Kazmierczak, N. P.; Hadt, R. G. Deconvolving Contributions to Decoherence in Molecular Electron Spin Qubits: A Dynamic Ligand Field Approach. *Chem.—Eur. J.* **2021**, *27*, 9482−9494. (c) Kazmierczak, N. P.; Xia, K. T.; Sutcliffe, E.; Aalto, J. P.; Hadt, R. G. A Spectrochemical Series for Electron Spin Relaxation. *J. Am. Chem. Soc.* **2025**, *147*, 2849−2859.
(41) (a) Goldbeck, R. A.; Dawes, T. D.; Milder, S. J.; Lewis, J. W.; Kliger, D. S. Measurement of Magnetic Circular Dichroism (MCD) on a Nanosecond Timescale. *Chem. Phys. Lett.* **1989**, *156*, 545−549. (b) Goldbeck, R. A.; Dawes, T. D.; Einarsdóttir, O.; Woodruff, W. H.; Kliger, D. S. Time-Resolved Magnetic Circular Dichroism Spectroscopy of Photolyzed Carbonmonoxy Cytochrome c Oxidase (Cytochrome Aa3). *Biophys. J.* **1991**, *60*, 125−134. (c) Shapiro, D. B.; Goldbeck, R. A.; Che, D.; Esquerra, R. M.; Paquette, S. J.; Kliger, D. S. Nanosecond Optical Rotatory Dispersion Spectroscopy: Application to Photolyzed Hemoglobin−CO Kinetics. *Biophys. J.* **1995**, *68*, 326−334. (d) Goldbeck, R. A.; Kim-Shapiro, D. B.; Kliger, D. S. Fast Natural and Magnetic Circular Dichroism Spectroscopy. *Annu. Rev. Phys. Chem.* **1997**, *48*, 453−479. (e) Esquerra, R. M.;

https://doi.org/10.1021/jacs.5c03783
J. Am. Chem. Soc. 2025, 147, 18424−18430

Goldbeck, R. A.; Kim-Shapiro, D. B.; Kliger, D. S. Fast Time-Resolved Magnetic Optical Rotatory Dispersion Measurements. 1. Mueller Analysis of Optical and Photoselection-Induced Artifacts. *J. Phys. Chem. A* **1998**, *102*, 8740−8748. (f) Chen, E.; Goldbeck, R. A.; Kliger, D. S. Nanosecond Time-Resolved Polarization Spectroscopies: Tools for Probing Protein Reaction Mechanisms. *Methods* **2010**, *52*, 3−11. (g) Kliger, D. S.; Chen, E.; Goldbeck, R. A. *Comprehensive Chiroptical Spectroscopy*; John Wiley & Sons, Ltd., 2011; Chapter 7, pp 179−201.

https://doi.org/10.1021/jacs.5c03783
J. Am. Chem. Soc. 2025, 147, 18424−18430